



OPEN Effect of plant ash incorporation on hydrologic processes of coarse-textured soils

Edouard J. Acuña¹ & Carlos A. Bonilla^{1,2,3,4}✉

Wildfires significantly affect soil hydrologic processes, particularly in coarse-textured soils common in fire-prone areas such as central Chile. This study evaluated the hydrological effects of incorporating plant-derived ash into coarse-textured soils using laboratory measurements and HYDRUS-1D modeling. Ashes from *Eucalyptus globulus* (exotic) and *Quillaja saponaria* (native) were incorporated at 4% by weight into sandy loam (SL) and sandy clay loam (SCL) soils, simulating mixing into the upper 5 cm of a 30 cm profile. Compared to soils without ash, *Q. saponaria* increased saturated water contents by 12% in SL and 9% in SCL, while saturated hydraulic conductivity (Ks) decreased by 82% in SL with *E. globulus* and by 69% in SCL with *Q. saponaria*. Ash effects were concentrated near the surface, at 2.5 cm depth, volumetric water content (θ) increased up to 42% in SL with *Q. saponaria* and 21% in SCL with *E. globulus* during the rainy season. Simulations showed that, for similar depths, ash-amended soils retained higher θ despite lower pressure heads (more negative h), indicating enhanced moisture availability. Rosetta-based scenarios overestimated θ , as confirmed by RMSE analysis. These results underscore the value of process-based modeling for assessing post-fire soil behavior and the hydrological role of ash incorporation.

Keywords Wildfire ash, HYDRUS-1D, Post-fire management, Soil hydrology, Soil water retention

Wildfires are becoming increasingly frequent and severe worldwide, especially in fire-prone countries such as Canada, Russia, and parts of Europe, along with several South American countries¹. This trend has been linked to warmer and drier conditions driven by climate change^{2,3}. One of the most concerning outcomes of wildfires is their impact on soil. The intense heat and loss of vegetation cover typically lead to increased erosion, reduced infiltration, and changes in soil physical and chemical properties^{4–8}. In particular, fire-induced soil hydrophobicity, organic matter degradation, and surface sealing processes enhance surface runoff and reduce the soil's ability to retain water^{9,10}.

A key component influencing post-fire soil hydrology is the presence of ash, defined as the mineral and partially charred organic residue that remains after vegetation combustion¹¹. Depending on its physical and chemical characteristics, ash can improve or degrade hydrological soil properties. For instance, coarse and less compact ash produced at lower combustion temperatures may increase infiltration rates due to higher saturated hydraulic conductivity¹², whereas fine-textured ash formed under high temperatures tends to clog soil pores and reduce hydraulic conductivity^{10,11}. The presence of surface ash can also promote crust formation, limiting infiltration and enhancing overland flow, particularly when combined with intense rainfall events^{10,13}. Additionally, the chemical composition of ash, including nutrients such as potassium, calcium, and magnesium, may temporarily enrich the soil or, conversely, pose contamination risks when mobilized into nearby water bodies^{5,14}.

The impact of ash on soil hydrological processes is highly context-dependent. Factors such as fire severity, ash depth and type, topography, and post-fire rainfall patterns, all modulate the soil's response^{9,15}. Furthermore, coarse-textured soils (such as sandy soils) cover vast global areas and are especially sensitive to post-fire disturbances due to their low water-holding capacity and high permeability¹⁶. In these soils, the incorporation of ash has been reported to improve field capacity, permanent wilting point, and plant available water^{12,17}. Nevertheless, research on how ash incorporation affects infiltration and other hydrological properties in coarse-

¹Departamento de Ingeniería Hidráulica y Ambiental, Pontificia Universidad Católica de Chile, Macul, Santiago, Chile. ²Department of Crop and Soil Science, Oregon State University, Corvallis, OR, USA. ³Hermiston Agricultural Research and Extension Center, Oregon State University, 2121 S 1st St, Hermiston, OR 97838, USA. ⁴Centro de Desarrollo Urbano Sustentable ANID/FONDAP/1523A0004, El Comendador 1916, Providencia, Santiago 7520245, Chile. ✉email: carlos.bonilla@oregonstate.edu

textured soils remains limited. This is particularly relevant in Mediterranean climate regions, such as central Chile, where these soils are widespread and frequently exposed to fire events.

Post-fire management practices vary in scale and effectiveness. Common strategies include mulching, reforestation, and the installation of erosion barriers¹⁸. Some approaches focus specifically on manipulating ash layers. For instance, manual raking or tillage can incorporate ash into the topsoil, reducing surface water repellency and stratification^{13,19}. However, it is essential to consider soil texture before implementing such interventions, as this property can strongly influence the risk of surface runoff and water ponding after ash incorporation²⁰. Coarse-textured soils may be more vulnerable to rapid water movement and erosion under these conditions, making the assessment of site-specific characteristics a critical component of post-fire management strategies.

Post-fire ash can act as both a nutrient source and a hydrological modifier, potentially enhancing water retention or reducing infiltration due to pore clogging or surface sealing^{3,15}. Moreover, when transported by wind or water, ash particles may carry heavy metals and polycyclic aromatic hydrocarbons, negatively impacting downstream aquatic ecosystems^{11,21}. These risks underscore the importance of understanding the fate and function of ash in soil and watershed systems, particularly following high-intensity fire events. Given the complexity of these interactions, hydrological models provide an invaluable tool for simulating and understanding post-fire soil processes under various management scenarios. HYDRUS-1D, a widely used software that solves the Richards' equation for water flow in unsaturated-saturated soils, has proven effective in evaluating the effects of incorporating soil amendments²². Modeling approaches offer unique advantages, such as assessing the influence of ash incorporation on soil water content, infiltration, and water fluxes that can be observed at specific soil depths, which are difficult to measure in a representative way in field conditions.

Most research has focused on comparing burned versus unburned conditions, with limited efforts to model the effects of post-fire management actions¹⁸, such as ash incorporation. This knowledge gap hinders the development of robust soil management strategies in fire-affected areas. Central Chile, a region with a Mediterranean climate characterized by recurrent summer droughts and high fire incidence, hosts two contrasting vegetation types strongly affected by wildfires: *Eucalyptus globulus*, one of the most widespread exotic plantation species, and *Quillaja saponaria*, a representative native tree of sclerophyllous forests. Their coexistence in fire-prone landscapes makes them particularly relevant for evaluating post-fire ash incorporation and its potential influence on soil hydrological processes. This is particularly relevant for coarse-textured soils, which dominate many areas within the Chilean Matorral ecoregion, where sandy loam and loamy textures are widespread²³. In this context, the present study hypothesizes that the superficial incorporation of ashes from *E. globulus* and *Q. saponaria* modifies the hydraulic parameters that control near-surface water dynamics in coarse-textured soils to different magnitudes, relative to soils without ash. To this end, this research aims to evaluate the impact of incorporating ashes derived from *E. globulus* and *Q. saponaria* into the hydrologic processes of two coarse-textured soils, using a methodology that combines experimental laboratory measurements with HYDRUS-1D modeling. Thus, this research contributes to a better understanding of how ash type and its incorporation influence soil water dynamics and supports the development of evidence-based strategies for enhancing soil recovery and hydrological resilience after wildfires.

Materials and methods

Research sites

The research was conducted in the semi-arid zone of Central Chile, encompassing areas within both the Valparaíso and Metropolitan Regions. In the Valparaíso Region, the first research area was in the commune of La Ligua (32.4608° S, 71.2478° W; 95 m above sea level [m.a.s.l.]). The second research area in the Metropolitan Region, in the commune of Melipilla (33.4819° S, 71.2804° W; 187 m.a.s.l.). Both areas exhibit Mediterranean climatic conditions, characterized by winter concentrated precipitation and a prolonged dry season. According to historical records, the La Ligua area has a mean annual temperature of 14.2 °C and an annual precipitation of 274 mm. Melipilla has a mean annual temperature of 14.4 °C and an annual precipitation of 407 mm²⁴.

Sampling of soils and characterization

Coarse-textured soils were collected from two research sites. The Sandy Loam (SL) soil from La Ligua represented a natural, non-cultivated condition without recent disturbances, corresponding to a native shrub-grassland community dominated by *Vachellia caven* (formerly *Acacia caven*). In contrast, the Sandy Clay Loam (SCL) soil from Melipilla represented an agricultural soil under recent tillage, characterized by the absence of standing crops or active roots systems at the time of sampling. Both soils are classified as *Ultic Haploxeralfs* of the Lo Vásquez series²⁵, which are derived from granitic rocks and found on hill slopes widely distributed across the coastal range in central Chile. The soil samples were collected at 0–15 cm depth by manual excavation with a steel shovel, air-dried at room temperature for four months, gently disaggregated, and sieved to ≤ 2 mm to obtain disturbed samples for laboratory analysis²⁵. In both soils, pH and electrical conductivity (EC) were determined in a 1:2.5 (W V⁻¹) soil to water suspension using a pH meter (Thermo Scientific, Orion Star A211) and a conductivity meter (Thermo Scientific, Orion Star A212). Particle size distribution was assessed using a PARIO soil texture analyzer²⁶, and organic matter content was determined by wet oxidation²⁷.

Ash production

To create a contrast between representative exotic and native species in Chile, ash materials were produced from *Eucalyptus globulus* (exotic) and *Quillaja saponaria* (native), both species widely distributed in south-central Chile^{28–30}. Leaves and small branches were collected, rinsed with distilled water, and air-dried at room temperature for three months. After drying, the moisture content was $6.26\% \pm 0.20$ for *Q. saponaria* and $9.10\% \pm 0.80$ for *E. globulus*. The dried plant material was then burned under controlled conditions, with thermocouples

used to monitor combustion temperatures. The maximum temperature reached during combustion for both species was approximately 500 °C. The resulting ash was sieved through a 2 mm mesh to separate fully combusted material (gray ash) from partially combusted residues (char), following the procedures suggested by Kim et al.¹⁰, Stoof et al.³¹, and Escudey et al.³². The remaining carbon content of ash samples was analyzed using a muffle furnace at 400 °C for 15 h to combust any residual carbon in ash samples³³. Ash materials showed differences in the remaining carbon content, which was $10.6 \pm 0.1\%$ for *Q. Saponaria* and $3.8 \pm 0.1\%$ for *E. globulus*. The gray ash was used to mix SL and SCL soils with ash samples and to generate the soil samples with incorporated ash.

Ash incorporation scenarios

The soil samples were gently packed in steel cylinders (250 cm³) using moderate pressure to achieve bulk densities of 1.53 g cm⁻³ (SL) and 1.56 g cm⁻³ (SCL), based on values obtained from laboratory compaction tests, and consistent with coarse-textured soils characterized by high sand content. Then, the packed soils were saturated by capillarity for one week using a solution prepared from boiled distilled water with CaCl₂ added, adjusted to match the soil electrical conductivity. Additionally, the ash samples from *E. globulus* and *Q. saponaria* were manually mixed with SL and SCL soils and packed into 250 cm³ steel cylinders. Bulk density was treated as a controlled variable, therefore, the same bulk densities used for the SL and SCL without ash were maintained for the ash-incorporated soil samples. Considering four replicates, measurements of saturated hydraulic conductivity (Ks) using a KSAT device (Meter[®]), and the water retention characteristics through HYPROP and WP4C devices (Meter Group, Pullman, WA, USA) were implemented. The soil water retention data were fitted using the unimodal van Genuchten model³⁴ and the software LABROS SoilView-Analysis (Version 5.0.5.0, Meter group). These measurements provided the α , n , θ_s , and θ_r parameters used as inputs for hydrological modeling in HYDRUS-1D. The scenarios of ash incorporation considered two coarse-textured soils (SL and SCL), two ash types (*E. globulus* and *Q. saponaria*) applied at a dose of 4% by weight (W W⁻¹), and five centimeters as ash incorporation depth. The ash dose selected corresponds to approximately 30 Mg ha⁻¹ of ash in the upper 5 cm of soil, which is consistent with realistic post-fire conditions reported for Eucalyptus forests, where ash deposits range between 6 and 34 Mg ha⁻¹ depending on fire severity³⁵. Moreover, this dose falls within the range of ash production expected in *E. globulus* plantations in Chile, where aboveground dry matter yields of 100–400 Mg ha⁻¹ at 12–18 years³⁶, can result in 20–40 Mg ha⁻¹ of ash, assuming conversion rates of 5–10% from plant material to ash. However, the total ash produced during a fire is largely determined by plant fractions and combustion completeness^{37,38}. For *Q. saponaria*, the same dose was applied to enable direct comparisons across both species and maintain methodological consistency. Therefore, the ash incorporation scenarios represent a realistic condition and enable the assessment of their hydrological impact under post-fire field conditions.

Simulation of soil hydrological processes for an average year

A one-year average soil hydrological simulation was conducted using the HYDRUS-1D software to evaluate four scenarios of ash incorporation. Meteorological data from 2019 to 2024 were obtained from nearby weather stations and used as input for the reference evapotranspiration (ET_o) calculation, which was determined using the Penman-Monteith equation³⁹. These historical climate records, including precipitation, net radiation, minimum and maximum air temperature, relative humidity, and wind speed, were retrieved from stations #320,063 (SL) and #330,111 (SCL) of the Chilean Meteorological Directorate database⁴⁰. A climatological average year was then generated by calculating the mean value for each calendar day (day 1 to day 365) across the six years (Fig. 1). This period was selected to capture recent interannual variability and trends in La Ligua and Melipilla research areas, ensuring that the input data reflect the current climatic conditions. In this context, the ongoing megadrought in central Chile since 2010 has redefined the regional climate baseline, leading to a 20–40% decrease in annual rainfall and increased evaporative demand⁴¹. These changes have significantly altered soil moisture regimes and introduced new land and water management challenges. Thus, this study does not focus on characterizing long-term climatic averages but instead simulates soil water dynamics under contemporary climatic conditions to evaluate scenarios of ash incorporation. Moreover, this approach preserved the daily resolution of climate variables while maintaining representativeness over the six years. All climate variables were adjusted to a daily time step, consistent with the temporal resolution specified in HYDRUS-1D for simulating transient water flow under daily atmospheric boundary conditions. These climatic inputs enabled a realistic simulation of soil water dynamics under both control and ash incorporation scenarios, supporting its applicability under post-fire conditions in the research areas.

HYDRUS-1D solves the Richards equation using the finite element method, allowing the representation of water flux in a porous medium with variable soil water content⁴². Given the post-fire context, plant transpiration was assumed to be negligible. Thus, soil evaporation was approximated as ET_o. The soil domain for modeling the hydrological processes in HYDRUS-1D was 30 cm, with observation nodes located at 2.5 cm, 10 cm, and 20 cm (Fig. 2). These depths were selected to encompass the soil zone with the highest hydrological relevance following wildfire and its biological significance, given that at least half of the global root biomass is typically concentrated within the upper 30 cm of soil⁴³. This layer plays a key role in early post-fire ecological succession, including root regrowth, microbial recolonization, and nutrient cycling, and is the central zone affected by ash deposition and changes in surface hydraulic properties^{44–46}. Therefore, modeling this portion of the profile enables a realistic assessment of the soil water dynamics that directly influence vegetation recovery and erosion potential after fires.

To provide a baseline reference using pedotransfer functions (PTFs), the SL and SCL soils' hydrological processes were also estimated using Rosetta Lite v1⁴⁷. The inputs for the model included sand, silt, and clay contents, and bulk density. This allowed for comparison with scenarios based on measured parameters, highlighting potential deviations when direct measurements are unavailable, a relevant consideration in post-fire contexts where soil data acquisition may be limited. Accordingly, for SL and SCL, the ash incorporation scenarios studied were: Control (soil without ash), E (4% of *E. globulus* ash at a depth of 5 cm), Q (4% of *Q.*

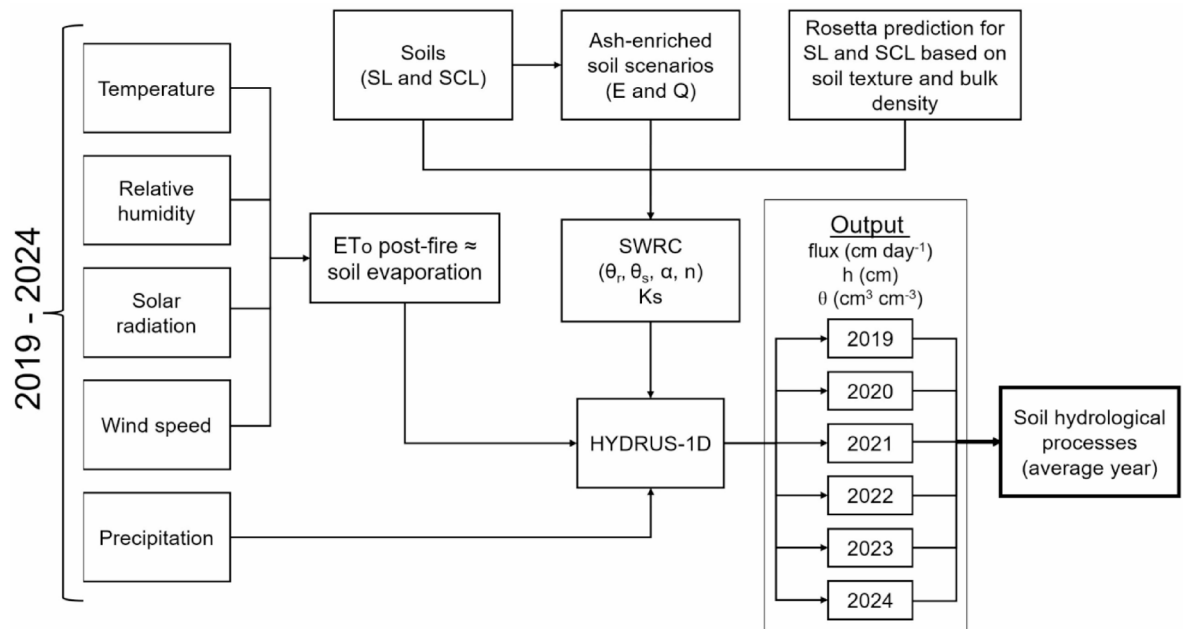


Fig. 1. Workflow to model average annual soil hydrological processes under different scenarios of post-fire ash incorporation.

saponaria ash at a depth of 5 cm), and Rosetta (R). The HYDRUS simulation incorporated an atmospheric boundary condition with surface runoff as the upper boundary and free drainage as the lower boundary condition. Simulation outputs over the six years included water flux (cm day⁻¹), pressure head (h; cm), and volumetric water content (θ ; cm³ cm⁻³). These outputs were averaged over the simulation period to represent the soil hydrological processes as a one-year average (365 days) under the four evaluated scenarios.

Data analysis

To evaluate the agreement among the Control, ash incorporation scenarios (E and Q), and the Rosetta estimates (R), the HYDRUS-1D outputs (flux, h, and θ) were compared using the root mean squared error (RMSE), defined as:

$$\text{RMSE} = \sqrt{\frac{1}{n} \sum_{i=1}^n (y_i - \hat{y}_i)^2} \quad (1)$$

where \hat{y} is the output value for the E, Q, or R scenarios, and y is the corresponding output value for the Control. RMSE is a widely accepted metric for assessing model performance, as it quantifies the average magnitude of the differences between predicted and reference values. It is used to compare how closely the water flux, h, and θ simulated under each scenario matched those from the Control. Moreover, RMSE retains the units of the analyzed variable, allowing for direct physical interpretation and meaningful comparisons across depths and variables. This feature is particularly relevant in soil hydrology, where differences in water flux (cm day⁻¹), h (cm), and θ (cm³ cm⁻³) must be interpreted.

All statistical analyses and figures were conducted using R⁴⁸ (version 4.4.2), employing the *tidyverse*⁴⁹ package for data processing, *ggplot2*⁵⁰ for data visualization, and *hydroGOF*⁵¹ to compute RMSE values. The tidyverse tools facilitated the organization and transformation of HYDRUS-1D outputs, while ggplot2 enabled the creation of comparative plots across scenarios. RMSE calculations using hydroGOF allowed for the quantitative assessment of deviations between the Control and ash incorporation or Rosetta scenarios.

Results and discussion

Properties of the soils

The initial characterization of both soils revealed sand contents exceeding 60% (Table 1). Regarding electrical conductivity (EC), both soils were classified as non-saline based on the threshold proposed for aqueous suspensions⁵². The SL soil exhibited a moderately acidic pH, whereas the SCL soil was neutral. Regarding water retention, field capacity (FC) values were similar for both soils. However, plant available water (PAW) was slightly higher in SL (PAW = 0.134 cm³ cm⁻³) than in SCL (PAW = 0.123 cm³ cm⁻³), due to the higher organic matter content in SL (2.0%) compared to SCL (1.5%). Nonetheless, both soils showed low levels of organic matter, consistent with the typical characteristics of Alfisols in the study area²⁵.

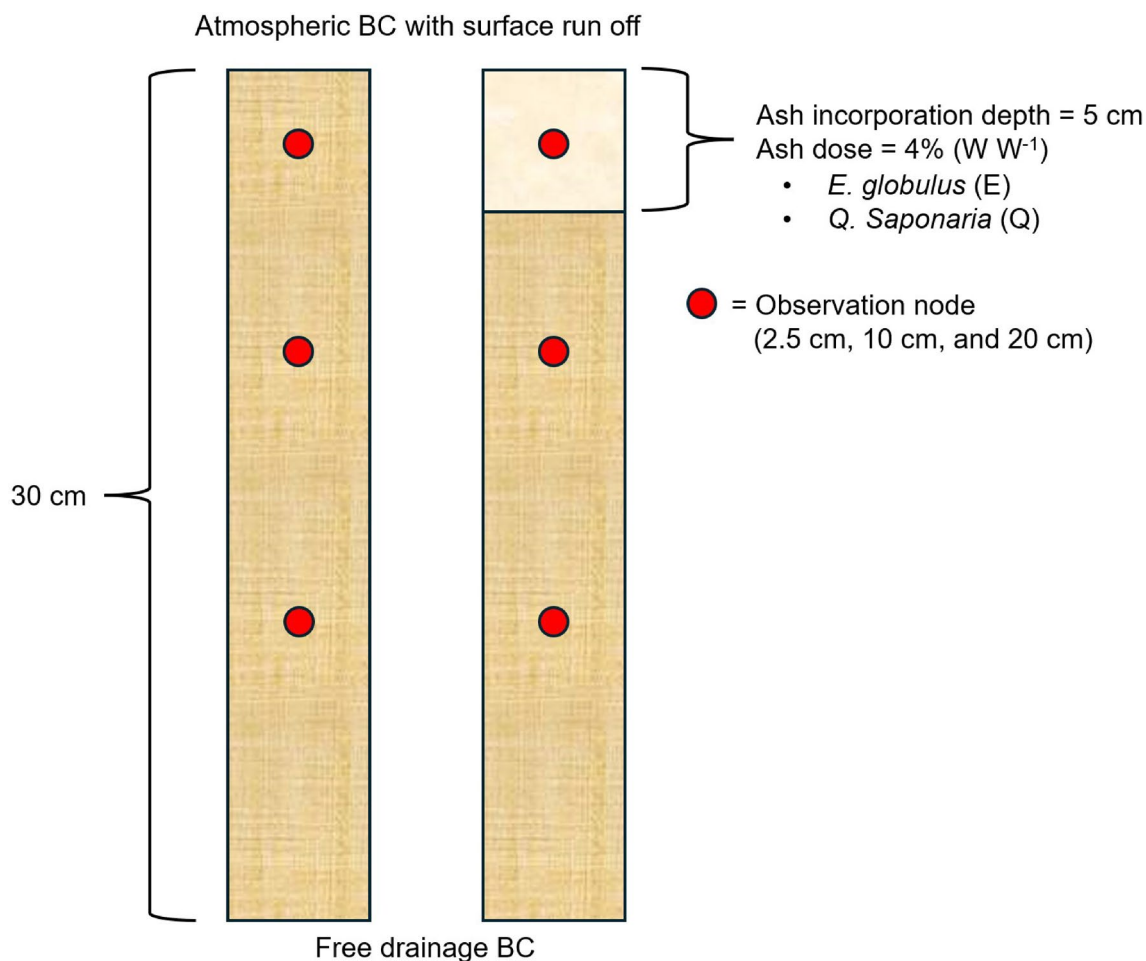


Fig. 2. Schematic representation of the soil domains simulated in HYDRUS-1D, illustrating boundary conditions (BC), ash incorporation scenarios (*E. globulus* and *Q. saponaria*), and observation node depths.

Parameter	Unit	Sandy Loam	Sandy Clay Loam
		(SL)	(SCL)
pH (1:2.5)	-	5.8	6.7
EC (1:2.5)	$\mu\text{S cm}^{-1}$	98.2	110.9
Sand	%	67	61
Silt	%	18	18
Clay	%	15	21
Field capacity	θ ($\text{cm}^3 \text{cm}^{-3}$)	0.190	0.189
Permanent wilting point	θ ($\text{cm}^3 \text{cm}^{-3}$)	0.056	0.066
Plant available water	θ ($\text{cm}^3 \text{cm}^{-3}$)	0.134	0.123
Organic matter	%	2.0	1.5

Table 1. Main properties of the coarse-textured soils used in this study.

Climatic conditions of research areas

The climatic data from La Ligua (SL) and Melipilla (SCL), corresponding to the 2019–2024 period, highlight the pronounced seasonality and interannual variability characteristic of the Mediterranean climate in Central Chile (Fig. 3). The total annual reference evapotranspiration (ET_o) ranged from 1,551 to 1,641 mm in La Ligua and 1,860 to 1,998 mm in Melipilla, reflecting the higher evaporative demand in the latter location. Precipitation exhibited greater variability between years, with the lowest annual totals observed in 2019 (60.1 mm in La Ligua; 67.5 mm in Melipilla) and the highest in 2023 (230.1 mm in La Ligua; 387.1 mm in Melipilla). Notably, precipitation was consistently lower than ET_o across both sites and all years. The temporal distribution of precipitation, concentrated in winter months, contrasts significantly with the persistent atmospheric demand

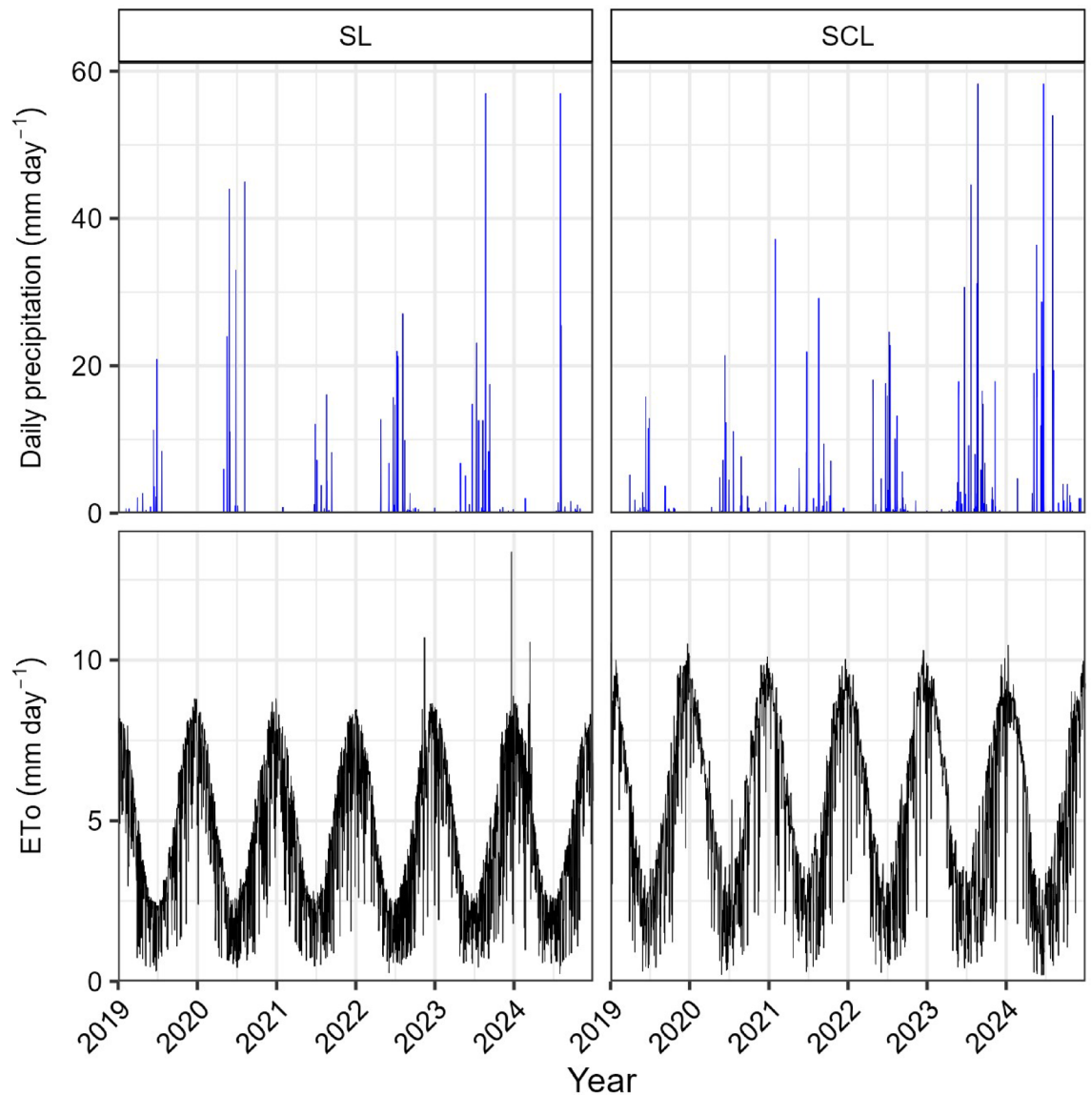


Fig. 3. Daily precipitation and reference evapotranspiration (ETo) from 2019 to 2024 for SL and SCL soils located in La Ligua (Valparaíso Region) and Melipilla (Metropolitan Region), respectively.

(ETo), which peaks during the dry season. According to historical records⁵³, this seasonal variance is further illustrated by the daily chance of precipitation, which peaks in late June (23% in Melipilla and 18% in La Ligua), and remains below 2% between November and March.

Meanwhile, the probability of clear or mostly clear skies exceeds 90% in both locations during summer, dropping to annual lows of 42% in Melipilla and 47% in La Ligua in midwinter. These patterns highlight stronger cloud cover and precipitation frequency during the cooler season, particularly in Melipilla. Supporting this, long-term climatological records show that Melipilla consistently exhibits higher average temperatures than La Ligua throughout the year, with summer maxima reaching 29.5 °C and winter minima around 4.6 °C, compared to 26.3 °C and 5.5 °C in La Ligua, respectively²⁴. Such conditions reinforce the prevailing water deficit and support management strategies after wildfires. Moreover, these climatic conditions are critical for the hydrological modeling of SL and SCL soils, as they directly influence the boundary conditions and temporal dynamics of water fluxes.

Soil hydraulic parameters and the effect of Ash incorporation

The Van Genuchten parameters (α , n , θ_r , and θ_s) and Ks experimentally measured for SL and SCL soils, with and without ash incorporation, are essential for modeling and understanding the unsaturated water dynamics. In SL, the α value decreased in both the E (0.013) and Q (0.014) treatments relative to the Control (0.018), indicating a delayed air entry point and potentially finer pores because of ash incorporation (Table 2). Similarly, n values decreased from 1.572 for the Control to 1.519 and 1.467 for E and Q scenarios, suggesting a more gradual slope of the water retention curve and a broader pore size distribution. A slight reduction in θ_r was observed, while

Soil	Scenario	α		n		θ_r		θ_s		K_s	
		(cm^{-1})		$(-)$		$(\text{cm}^3 \text{cm}^{-3})$		$(\text{cm}^3 \text{cm}^{-3})$		(cm day^{-1})	
SL	Control	0.018	± 0.001	1.572	± 0.047	0.032	± 0.004	0.437	± 0.011	75.3	± 5.620
	E	0.013	± 0.001	1.519	± 0.055	0.028	± 0.009	0.442	± 0.005	13.3	± 1.930
	Q	0.014	± 0.000	1.467	± 0.023	0.025	± 0.007	0.489	± 0.014	14.0	± 3.490
	R	0.0292		1.4158		0.0502		0.3775		28.37	
SCL	Control	0.021	± 0.001	1.552	± 0.036	0.050	± 0.003	0.449	± 0.010	107.8	± 5.980
	E	0.011	± 0.001	1.574	± 0.017	0.046	± 0.002	0.447	± 0.007	23.8	± 2.950
	Q	0.014	± 0.002	1.491	± 0.071	0.037	± 0.013	0.491	± 0.006	33.3	± 1.440
	R	0.0231		1.3752		0.0600		0.3930		19.87	

Table 2. Van Genuchten parameters (α , n , θ_r , and θ_s) and saturated hydraulic conductivity (K_s) according to different scenarios of Ash incorporation in coarse-textured soils (SL and SCL). Values are means \pm standard errors ($n = 4$). SL: Sandy Loam soil. SCL: Sandy Clay Loam soil. E: incorporation of 4% *E. globulus* ashes. Q: incorporation of 4% *Q. saponaria* ashes. K_s : saturated hydraulic conductivity. The parameters α , n , θ_r , and θ_s were experimentally determined from four replicated water retention curves, fitted using the unimodal van Genuchten model, for both SL and SCL soils under the Control (no ash) and ash incorporation scenarios (E and Q). R: Parameters estimated using Rosetta Lite v1.1, based on experimentally determined texture and bulk density.

θ_s slightly increased with ash incorporation, rising from $0.437 \text{ cm}^3 \text{ cm}^{-3}$ in the Control to $0.442 \text{ cm}^3 \text{ cm}^{-3}$ in E, and further increasing to $0.489 \text{ cm}^3 \text{ cm}^{-3}$ in the Q scenario, indicating a fostering of total porosity. However, K_s was markedly reduced from 75.3 cm day^{-1} in the control to 13.3 cm day^{-1} and 14.0 cm day^{-1} for the E and Q treatments, respectively. This marked K_s reduction reflects partial pore occlusion induced by fine ash particles, which may reduce soil macropore connectivity.

In SCL, α also decreased following ash incorporation, with values of 0.011 for E and 0.014 for Q, compared to 0.021 in the Control. However, only the Q treatment led to a reduction in the n parameter. Moreover, the θ_s value increased only under the Q scenario ($0.491 \text{ cm}^3 \text{ cm}^{-3}$) compared to the Control ($0.449 \text{ cm}^3 \text{ cm}^{-3}$), suggesting enhanced total porosity due to the inherently higher porosity of *Q. saponaria* ash compared to *E. globulus* ash, which may reflect the higher residual carbon content observed in the *Q. saponaria* ashes. As for SL, a pronounced decline in K_s was observed, from $107.8 \text{ cm day}^{-1}$ in the control to 23.8 cm day^{-1} (E) and 33.3 cm day^{-1} (Q), indicating a reduction in water transmission capacity under saturated conditions. These observations are consistent with recent evidence showing that wildfire ash is a porous and heterogeneous material, often exhibiting high specific surface area and void ratios, which can enhance water retention^{9,14} and influence the shape of the soil water retention curve by reducing α and n values.

Overall, fine particulate materials such as gray ash, wood ash, and analogous amendments can reduce K_s through surface sealing, crust formation, and partial pore occlusion^{10,11,20}. These effects, often accentuated by the expansive nature of ashes, have been associated with altered soil structure and diminished infiltration in finer-textured soils³¹. In this study, the minimum K_s values measured after ash incorporation in SL ($13.3 \pm 1.93 \text{ cm day}^{-1}$) and SCL ($28.3 \pm 2.95 \text{ cm day}^{-1}$) remained within the moderately high class according to USDA guidelines⁵⁴, indicating that coarse-textured soils subjected to ash incorporation maintain a high capacity to transmit water under saturated conditions. This supports the notion that, even with the addition of fine ash, pore clogging is not sufficient to block infiltration or cause surface ponding in coarse-textured soils, as demonstrated in pure sand experiments²⁰. The management implications of these findings differ according to land use. In natural forests and monoculture plantations, incorporating ash into the upper soil layer (hand raking or scarification) may reduce surface sealing and mitigate post-fire runoff and erosion. In addition, hand raking can partially alleviate the hydrophobic effects induced by certain ashes by mixing affected surface soil with deeper layers, although it must be combined with mulching to avoid increasing erodibility¹⁹. The effectiveness of these treatments depends on ash characteristics, since darker ashes may enhance infiltration while lighter ashes can promote surface sealing¹⁸. In agricultural soils, ash incorporation has shown to increase FC and PAW, particularly in coarse-textured soils, where analogous amendments such as wood ash and biochar improve pore size distribution and reduce bulk density^{17,55–58}. Beyond hydrological benefits, ashes contribute to soil fertility by supplying calcium, magnesium, potassium, and phosphorus, neutralizing soil acidity and enhance cation exchange capacity^{14,59,60}. However, the magnitude of these positive effects depends on both ash dose and soil type. Moderate applications can improve nutrient status and water retention, whereas excessive doses may decrease K_s ⁵⁵ or induce temporary increases in pH and salinity, effects that are especially critical in Mediterranean sandy soils^{61,62}.

The results indicate that ash incorporation involves hydrologic benefits as well some risks, which can differ between plant species. Nevertheless, accurately capturing these processes in modeling frameworks remains challenging. The Rosetta-derived parameters, estimated from soil texture and bulk density, tended to underestimate K_s , θ_s , and n , while overestimating α and θ_r for SL and SCL under the Control scenario. These inconsistencies emphasize the limitations of PTFs in accurately predicting hydraulic parameters, particularly when applied to soils that have undergone disturbances not directly reflected in input variables such as texture and bulk density. In this regard, even high application of ash (up to $15\% \text{ W W}^{-1}$), considerably greater than the 4% used in this study, has not affected soil texture³¹. This observation highlights a critical limitation in

relying solely on texture-based PTFs for predicting the hydraulic processes of soils, whether with or without ash incorporation. The Control scenario could not be reliably reproduced in this study despite having accurate texture and bulk density data. Consequently, measured hydraulic parameters should be prioritized in studies involving soil amendments such as ash, where traditional input variables may fail to capture control scenarios. Overall, incorporating ashes from *E. globulus* and *Q. saponaria* modified key hydraulic properties of both coarse-textured soils. These changes will affect infiltration, water retention, and drainage dynamics because of ash incorporation management, whether through tillage or hand raking practices. Thus, the experimental parameters presented here provide realistic inputs for HYDRUS-1D simulations, allowing improved prediction of soil hydrological responses to post-fire ash incorporation under Mediterranean climate conditions. However, it is important to note that these experiments and simulations have been conducted under controlled laboratory conditions with soil hydraulic parameters obtained from packed soils, which simplifies field variability, but allows isolating the effects of ash incorporation on soil. In addition, this evaluation was limited to a single ash dose, two ash types, and two coarse-textured soils, providing a realistic yet necessarily restricted set of post-fire scenarios. These considerations highlight the need for further research under field conditions and across a broader range of soils and ash incorporation scenarios, including the evaluation of spatial variability in water flow through advanced modeling approaches such as HYDRUS-3D.

Seasonal water flux dynamics

The simulations of one average year of soil hydrological processes using HYDRUS-1D highlighted differences among ash incorporation scenarios and water flow predictions based on Rosetta's pedotransfer functions. According to the vertical water fluxes in Fig. 4, all scenarios exhibited a clear seasonal pattern, characterized by upward fluxes during the summer months (January to March) and downward fluxes during the winter (mainly between May and August), corresponding to the rainfall season in central Chile. This dynamic was consistent in SL and SCL soils, although with varying magnitudes depending on the ash incorporation scenario and the evaluated depth.

In the SL soil, water fluxes at 2.5 cm depth under the Control, E, and Q scenarios followed similar patterns, with upward movement during the dry months and moderate percolation during winter. However, the scenarios involving ash incorporation (E and Q) tended to exhibit slightly more negative values during winter than the Control (e.g., average August fluxes were -0.0760 in Control, -0.0796 in E, and -0.0797 in Q), suggesting that ash addition may have slightly increased soil permeability. At 10 cm, the E and Q scenarios showed slightly reduced percolation compared to the Control during June, indicating a transient improvement in water retention. However, in other winter months (e.g., May and July), the behavior was similar across scenarios, with E and Q showing slightly more negative flux values than Control. At 20 cm depth, differences among the Control, E, and Q scenarios were minimal, indicating a limited influence of ash incorporation at this depth. Additionally, a general decline in flux magnitude with increasing depth was observed across all scenarios.

In the SCL soil, more intense flux values than SL were observed, particularly during the months of highest precipitation. At 2.5 cm, the Control, E, and Q scenarios exhibited high downward fluxes in June and July, with similar values between scenarios. However, at 10 cm depth, E and Q treatments tended to reduce fluxes in winter compared to the Control (e.g., average June flux: -0.1075 in E vs. -0.1133 in Control). At 20 cm, the scenarios involving ash incorporation also showed a slight reduction in downward flux relative to the Control, with more marked differences during the months of highest recharge (June to August). These results suggest that ash incorporation in SCL soil may enhance water retention at greater depths.

The Rosetta scenario consistently produced more negative water fluxes than the other treatments across both soils and at all depths. This tendency was especially pronounced in the SCL soil, where winter flux values under Rosetta were the most negative in the simulation (reaching -0.1179 in June at 2.5 cm). This greater water loss suggests that flux estimates generated using Rosetta may underestimate the water retention capacity of the coarse-textured soils evaluated. This represents a scenario less reflective of the actual initial conditions of SL and SCL soils without ash incorporation.

Ash effects on soil moisture dynamics

The volumetric water content simulations over an average year revealed apparent differences in the hydrological processes of ash-incorporated soil scenarios compared to the Control. These differences were more evident in the uppermost soil layer (2.5 cm), particularly during the winter months (June to August), corresponding to the rainy season in central Chile. Overall, the influence of ash incorporation diminished with depth, confirming that its effects are concentrated near the soil surface.

Incorporating *E. globulus* and *Q. saponaria* ashes in the SL soil increased water retention at 2.5 cm depth relative to the Control. For instance, during July, the Control scenario averaged a $\theta = 0.1099 \text{ cm}^3 \text{ cm}^{-3}$, whereas it reached $\theta = 0.1377 \text{ cm}^3 \text{ cm}^{-3}$ and $\theta = 0.1566 \text{ cm}^3 \text{ cm}^{-3}$ in the E and Q scenarios, respectively. This pattern suggests enhanced near-surface water retention is possible, resulting from the physical effects of fine ash particles, such as increased porosity and specific surface area. Notably, water retention of fully combusted ash, as the ash materials used in this research, far exceeded that of partially combusted char³¹, highlighting the role of combustion degree in modulating soil hydrological processes. The Q scenario consistently presented higher water content than the E scenario, which aligns with its higher remaining carbon content of this ash material, reinforcing the idea that post-fire carbon dynamics play a critical role in soil functions².

At 10 cm depth, although differences among scenarios were less pronounced, a slight trend toward improved water retention was observed. During August, the Control scenario reached an average of $\theta = 0.1381 \text{ cm}^3 \text{ cm}^{-3}$, whereas the E and Q treatments attained slightly higher average values of $\theta = 0.1405$ and $0.1394 \text{ cm}^3 \text{ cm}^{-3}$, respectively. These results suggest a moderate downward influence of the ash, possibly due to water redistribution within the soil profile. However, the E and Q scenarios exhibited values like the Control during the remaining

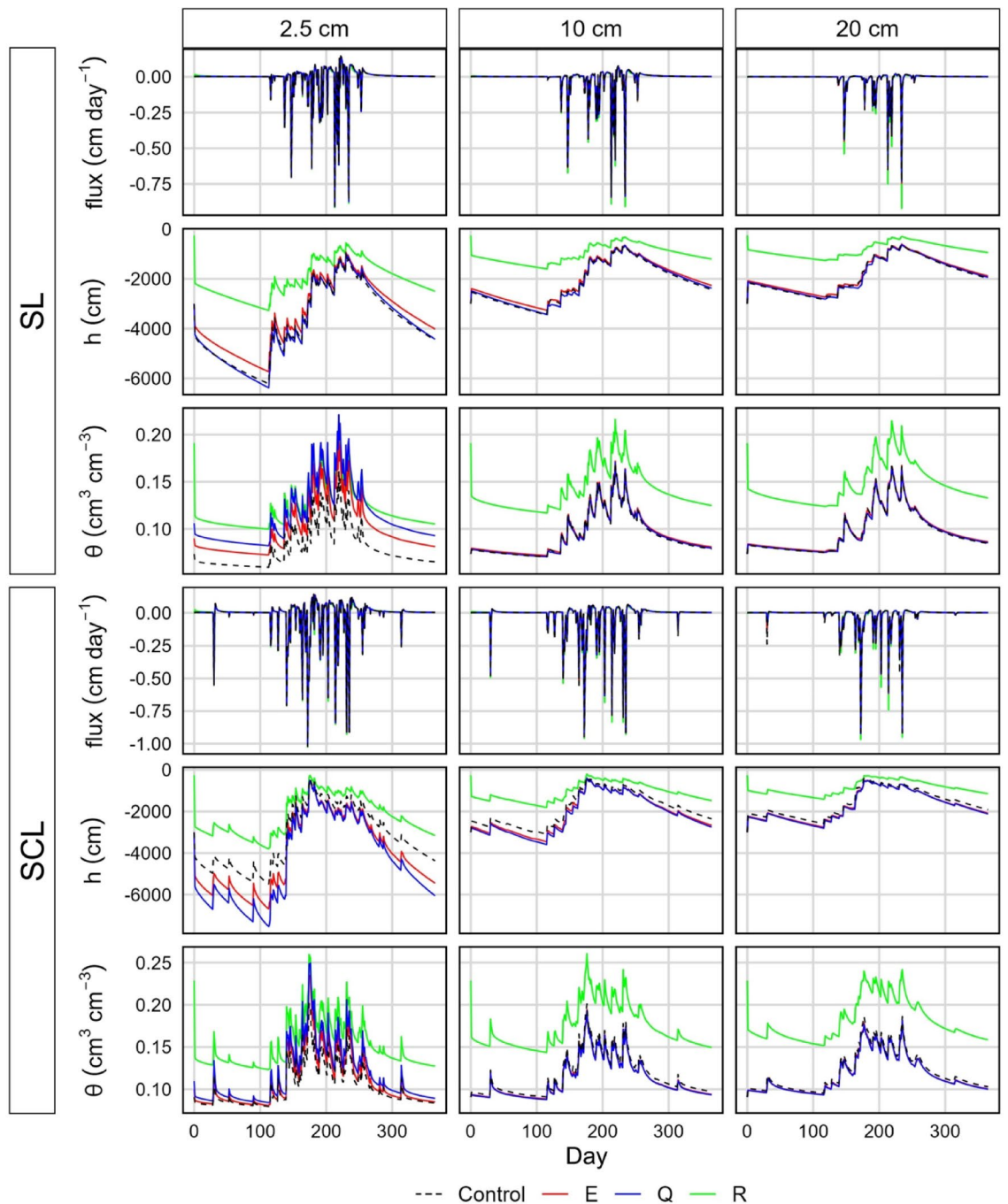


Fig. 4. Simulated flux (cm day^{-1}), pressure head (h ; cm), and volumetric water content (θ ; $\text{cm}^3 \text{cm}^{-3}$) at three soil depths (2.5 cm, 10 cm and 20 cm) under average annual climatic conditions. Estimates are for SL and SCL soils, considering different post-fire ash incorporation scenarios and Rosetta prediction.

winter months. At 20 cm depth, the volumetric water content in the E and Q scenarios remained slightly lower than in the Control throughout the year.

The SCL soil exhibited a similar but more pronounced response to ash incorporation. At 2.5 cm depth, water content under the Q treatment reached an average $\theta = 0.1572 \text{ cm}^3 \text{cm}^{-3}$ in July, compared to $\theta = 0.1305 \text{ cm}^3 \text{cm}^{-3}$ in the Control, reinforcing the role of ash in enhancing water retention under wetter conditions (winter months in Central Chile). This effect was particularly relevant in SCL (compared to SL) due to the synergistic interaction between the finer soil texture and ash incorporation. At 10 cm depth, the Control, E, and Q scenarios presented similar average values during the wet season (e.g., August: 0.1487, 0.1436, and 0.1434 $\text{cm}^3 \text{cm}^{-3}$, respectively). Nonetheless, the scenarios of ash incorporation maintained slightly higher retention during dry months, indicating a buffering effect under soil moisture decline. At 20 cm depth, differences in volumetric water content between scenarios were irrelevant throughout the year.

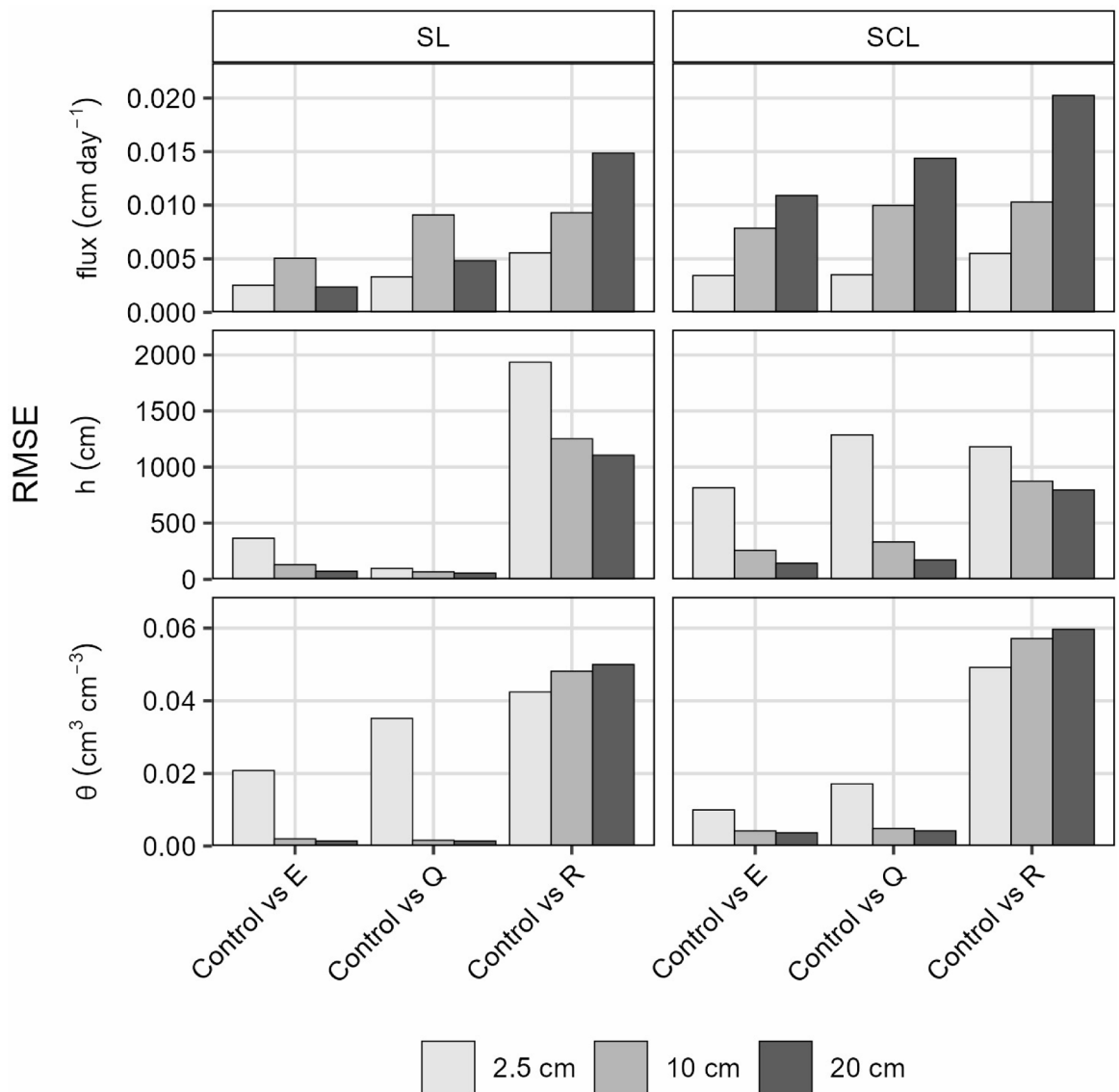


Fig. 5. Root mean square error (RMSE) of simulated flux (cm day^{-1}), pressure head (h ; cm), and volumetric water content (θ ; $\text{cm}^3 \text{cm}^{-3}$) at three depths (2.5 cm, 10 cm and 20 cm), comparing post-fire ash incorporation scenarios and Rosetta (R) prediction.

During the winter months, the Control scenario generally exhibited slightly higher water contents than the E and Q scenarios, suggesting that the influence of ash incorporation did not extend significantly beyond the amended layer. This pattern is expected with or without active ash management, as post-fire ash layers typically affect only the upper 5 cm of the soil profile⁹. Nevertheless, the observed improvements in shallow soil water retention may help mitigate the negative impacts of wildfires on multiple levels of soil organization, including structure, porosity, infiltration, thermal regime, and water storage⁶³. In this context, ash incorporation could partially counteract the decline in available water content commonly associated with repeated fire events⁶⁴. However, fire-induced phenomena such as soil hydrophobicity may offset these benefits, depending on ash composition and soil texture⁵. Furthermore, when ash is deposited directly onto the soil surface, it may clog and seal soil pores, reducing infiltration capacity⁴⁵. This underscores the importance of implementing appropriate ash management strategies. Complementary practices such as mulching should also be considered, as they have demonstrated a strong capacity to reduce overland flow and soil erosion¹⁵.

Particularly, in both SL and SCL soils, the differences observed in the trends between h and θ values at 2.5 cm depth between scenarios were attributed to the nonlinearity of the relationship between these parameters, as described by the van Genuchten model³⁴. Ash incorporation enhanced water retention, as evidenced by higher θ values in the E and Q scenarios at similar pressure heads compared to the Control. Accordingly, the Control scenario exhibited less negative h values, confirming that ash-amended soils retained more water at lower matric potentials. This behavior indicates enhanced soil water availability near the surface. It aligns with the physical

characteristics of ash-enriched soils, such as increased specific surface area and microporosity, contributing to improved water retention^{11,31}.

The Rosetta-derived scenario (R), based on pedotransfer functions, consistently overestimated the θ across all depths and months. These values exceeded those of experimental scenarios, indicating that PTFs may not adequately capture the hydrological processes of SL and SCL soils (without ash incorporation). Therefore, while useful for baseline estimations, Rosetta-derived predictions should be interpreted cautiously, and experimentally derived hydraulic parameters should be preferred when modeling ash-incorporated soil conditions.

RMSE comparison across Ash scenarios

The RMSE was employed to quantify the deviation of each ash incorporation scenario (E and Q), as well as the Rosetta-based estimation (R), relative to the Control scenario for each variable simulated by HYDRUS-1D (water flux, h , and θ). Despite traditional applications where RMSE is used to compare model predictions against observed data, this study used RMSE as a metric to evaluate the consistency of hydrological simulations by comparing each scenario with the Control (SL or SCL soils without ash incorporation). This approach enables the assessment of how ash incorporation or PTFs modeling alters the prediction of soil hydrological dynamics. Furthermore, RMSE is sensitive to large deviations, meaning that peak values or extreme simulation fluctuations can disproportionately affect the error metric. For example, significant differences in h between the Control and Rosetta scenarios contributed to higher RMSE values for this comparison (Fig. 5). Conversely, the Q scenario consistently produced lower RMSE values across variables and depths, indicating a closer alignment with the Control and minor discrepancies throughout the simulation period.

In the SL soil, the E scenario exhibited RMSE values for h of 363.8, 128.5, and 73.2 cm at 2.5, 10, and 20 cm depths, respectively, while the Q scenario showed lower RMSEs (97.9, 67.1, and 56.0 cm). The Rosetta scenario yielded markedly higher RMSEs (1936.0, 1252.6, and 1105.8 cm), reflecting substantial deviations in simulated water retention behavior. Similar trends were observed for θ and flux, with the Q scenario achieving the best agreement. In the SCL soil, RMSE values for h reached 815.7 (E), 1286.3 (Q), and 1180.8 cm (R) at 2.5 cm depth, while Rosetta again consistently produced the highest discrepancies. Overall, the systematic overestimation of θ by Rosetta was quantitatively confirmed through the RMSE analysis. This highlights the value of RMSE as a diagnostic tool for identifying discrepancies among simulation scenarios and assessing how different ash incorporation scenarios affect soil water dynamics.

Conclusions

This study evaluated the incorporation of *E. globulus* and *Q. saponaria* ashes (4% by weight) into the upper 5 cm of two coarse-textured soils and its effects on key soil hydraulic properties (including α , n , θ_s , and K_s), which are critical inputs for modeling soil hydrological responses under Mediterranean climate conditions. HYDRUS-1D simulations showed that ash effects were concentrated near the soil surface and were most evident at 2.5 cm depth during the rainy season. Ash incorporation enhanced θ at shallow depths despite lower h , particularly in the *Q. saponaria* scenario, which was associated with higher residual carbon content and porosity. This inverse relationship between θ and h indicated increased water availability at the surface, consistent with the higher specific surface area and microporosity of ash-enriched soils. Across both SL and SCL soils, the Rosetta-based scenario consistently overestimated θ and h at three soil depths, demonstrating the limitations of PTFs' texture-based approach. RMSE comparisons confirmed that experimental ash incorporation scenarios more closely matched the Control than Rosetta predictions. These findings underscore the importance of using experimentally measured hydraulic parameters when modeling post-fire hydrological processes, particularly in ash incorporation scenarios where soil texture remains unaltered, but soil hydraulic properties are significantly modified. Integrating modeling and experimental approaches provides a robust framework for evaluating ash management strategies and guiding an effective hydrological restoration of coarse-textured soils affected by fires.

Data availability

Data will be made available on request. Please contact the corresponding author.

Received: 19 May 2025; Accepted: 31 December 2025

Published online: 02 February 2026

References

- Kala, C. P. Environmental and socioeconomic impacts of forest fires: A call for multilateral Cooperation and management interventions. *Nat. Hazards Res.* **3**, 286–294 (2023).
- Jones, M. W. et al. State of Wildfires 2023–2024. *Earth Syst. Sci. Data*, **16**, 3601–3685 (2024). <https://doi.org/10.5194/essd-16-3601-2024>
- Verkaik, I. et al. Fire as a disturbance in mediterranean climate streams. *Hydrobiologia* **719**, 353–382 (2013). <https://doi.org/10.1007/s10750-013-1463-3>
- Girona-García, A., Vieira, D., Doerr, S., Panagos, P. & Santín, C. Into the unknown: the role of post-fire soil erosion in the carbon cycle. *Glob Chang. Biol* **30**, e17354 (2024).
- Moazeni, S. & Cerdà, A. The impacts of forest fires on watershed hydrological response. A review. *Trees, Forests and People*, **18**, (2024). <https://doi.org/10.1016/j.tfp.2024.100707>
- Melej, M. J. et al. Changes in macroaggregate stability as a result of wetting/drying cycles of soils with different organic matter and clay contents. *Geoderma* **448**, 116965 (2024). <https://doi.org/10.1016/j.geoderma.2024.116965>
- Aedo, S. A. & Bonilla, C. A. A numerical model for linking soil organic matter decay and wildfire severity. *Ecol Modell* **447**, 109506 (2021).
- Martínez, S. I., Contreras, C. P., Acevedo, S. E. & Bonilla, C. A. Unveiling soil temperature reached during a wildfire event using ex-post chemical and hydraulic soil analysis. *Science Total Environment* **822**, 153654 (2022).
- Wirth, X. et al. *Wildfire Ash Composition Eng. Behav.* doi:<https://doi.org/10.1061/JGGEFK>. (2024).

10. Kim, T., Lee, J., Lee, Y. E. & Im, S. Exploring the Role of Ash on Pore Clogging and Hydraulic Properties of Ash-Covered Soils under Laboratory Experiments. *Fire*, **5**, (2022).
11. Bodí, M. B. et al. Wildland fire ash: Production, composition and eco-hydro-geomorphic effects. *Earth Sci. Rev.* **130**, 103–127 (2014). <https://doi.org/10.1016/j.earscirev.2013.12.007>
12. Kuzyakov, Y., Merino, A. & Pereira, P. Ash and fire, char, and Biochar in the environment. *Land. Degrad. Dev.* **29**, 2040–2044 (2018).
13. Wittenberg, L., van der Wal, H., Keesstra, S. & Tessler, N. Post-fire management treatment effects on soil properties and burned area restoration in a wildland-urban interface, Haifa fire case study. *Science Total Environment* **716**, (2020).
14. Sánchez-García, C. et al. Chemical characteristics of wildfire Ash across the Globe and their environmental and socio-economic implications. *Environ Int* **178**, 108065 (2023).
15. Pereira, P., Francos, M., Brevik, E. C., Ubeda, X. & Bogunovic, I. Post-fire soil management. *Curr. Opin. Environ. Sci. Health.* **5**, 26–32 (2018). <https://doi.org/10.1016/j.coesh.2018.04.002>
16. Yost, J. L. & Hartemink, A. E. Soil organic carbon in sandy soils: A review. In *Advances in Agronomy*, **158**, 217–310 (Academic Press Inc.) (2019).
17. Razzaghi, F., Obour, P. B. & Arthur, E. Does biochar improve soil water retention? A systematic review and meta-analysis. *Geoderma*. **361**, (2020). <https://doi.org/10.1016/j.geoderma.2019.114055>
18. Zema, D. A. Postfire management impacts on soil hydrology. *Curr. Opin. Environ. Sci. Health.* **21**, (2021). <https://doi.org/10.1016/j.coesh.2021.100252>
19. USDA-NRCS. After the Fire - Hand Raking. Natural Resources Conservation Service. U.S. Department of Agriculture. (2024). https://www.nrcs.usda.gov/sites/default/files/2024-07/AtF-Hand_Raking-2020.pdf
20. Stoof, C. R. et al. Can pore-clogging by Ash explain post-fire runoff? *Int. J. Wildland Fire.* **25**, 294–305 (2016).
21. Robinne, F. N. et al. Scientists' warning on extreme wildfire risks to water supply. *Hydrol Process* **35**, e14086 (2021).
22. Yang, Y. et al. The applicability of HYDRUS-1D to infiltration of water-repellent soil at different depths. *European J. Soil. Science Preprint at.* <https://doi.org/10.1111/ejss.13100> (2021).
23. Dinamarca, D. I., Galleguillos, M. & Seguel, O. & Faúndez Urbina, C. CLSoilMaps: A National soil gridded database of physical and hydraulic soil properties for Chile. *Sci Data* **10**, 630 (2023).
24. Santibañez, F. *Atlas Agroclimático De Chile. Tomo III: Regiones De Valparaíso, Metropolitana, O'Higgins Y Del Maule* (Universidad de Chile. Facultad de Ciencias Agronómicas, 2017).
25. CIREN. *Estudio Agrológico. Descripciones De Suelos Materiales Y Símbolos: V Región. (Soil Survey, Soil Descriptions, Materials and Symbols: V Región). Publicación No. 116 (in Spanish)* (Centro de Información de Recursos Naturales, 1997).
26. Durner, W., Iden, S. C. & von Unold, G. The integral suspension pressure method (ISP) for precise particle-size analysis by gravitational sedimentation. *Water Resour. Res.* **53**, 33–48 (2017).
27. Walkley, I. A. & Black, I. An examination of the Degtjareff method for determining soil organic matter, and a proposed modification of the chromic acid Titration method. *Soil. Sci.* **37**, 29–38 (1934).
28. Braun, A. C., Faßnacht, F., Valencia, D. & Sepulveda, M. Consequences of land-use change and the wildfire disaster of 2017 for the central Chilean biodiversity hotspot. *Reg. Environ. Change.* **21**, 1–22 (2021).
29. Letelier, L., Valderrama, A., Stoll, A. & García-González, R. González-Rodríguez, A. Patterns of composition, richness and phylogenetic diversity of Woody plant communities of Quillaja saponaria Molina (Quillajaceae) in the Chilean sclerophyllous forest. *Gayana Bot.* **46**, 2017 (2017).
30. McWethy, D. B. et al. Landscape drivers of recent fire activity (2001–2017) in south-central Chile. *PLoS ONE*, **13**, (2018). <https://doi.org/10.1371/journal.pone.0201195>
31. Stoof, C. R., Wesseling, J. G. & Ritsema, C. J. Effects of fire and Ash on soil water retention. *Geoderma* **159**, 276–285 (2010).
32. Escudey, M., Arancibia-Miranda, N., Pizarro, C. & Antilén, M. Effect of Ash from forest fires on leaching in volcanic soils. *Catena (Amst)*. **135**, 383–392 (2015).
33. Burns, K. A. *The Effective Viscosity of Ash-Laden Flows*. The University of Montana, Graduate Student Theses, Dissertations, & Professional Papers, (2007).
34. van Genuchten, M. A closed-form equation for predicting the hydraulic conductivity of unsaturated soils. *Soil Sci. Soc. Am. J.* **44**, 892–898 (1980).
35. Santín, C., Doerr, S. H., Otero, X. L. & Chafer, C. J. Quantity, composition and water contamination potential of Ash produced under different wildfire severities. *Environ. Res.* **142**, 297–308 (2015).
36. Corvalán, P. & Hernández, J. *Tablas De Rendimiento En Biomasa Aérea En Pie Para Plantaciones De Eucalyptus Globulus En Chile. Facultad De Ciencias Forestales Y De La Conservación De La Naturaleza* (Universidad de Chile, 2012).
37. Muhdi, Sahar, A., Hanafiah, D. S., Zaitunah, A. & Nababan, F. W. B. Analysis of biomass and carbon potential on eucalyptus stand in industrial plantation forest, North Sumatra, Indonesia. In *IOP Conference Series: Earth and Environmental Science*, **374**, (Institute of Physics Publishing, 2019).
38. Odziejewicz, J. I., Wolejko, E., Wydro, U. & Wasil, M. & Jabłońska-Trypuć, A. Utilization of Ashes from Biomass Combustion. *Energies*, **15**, (2022). <https://doi.org/10.3390/en15249653>
39. Allen, R. G., Pereira, L. S., Raes, D. & Smith, M. *Evapotranspiración Del Cultivo: Guías Para La Determinación De Los Requerimientos De Agua De Los Cultivos (Estudio FAO Riego Y Drenaje N° 56)* (Organización de las Naciones Unidas para la Agricultura y la Alimentación (FAO), 2006).
40. DMC. Portal de Servicios Climáticos V.3.11. (2025). <https://climatologia.meteochile.gob.cl/>
41. Garreaud, R. et al. *Hyperdroughts in Central Chile: Drivers, Impacts and Projections.* <https://egusphere.copernicus.org/preprints/2025/egusphere-2025-517/> (2025). <https://doi.org/10.5194/egusphere-2025-517>
42. Šimúnek, J., Šejna, M., Saito, H., Sakai, M. & van Th, M. *The HYDRUS-1D Software Package for Simulating the One-Dimensional Movement of Water, Heat, and Multiple Solutes in Variably-Saturated Media.* (2018).
43. Schenk, H. J. & Jackson, R. B. The global biogeography of roots. *Ecol. Monogr.* **72**, 311–328 (2002).
44. Neary, D., Ryan, K. & DeBano, L. Wildland fire in ecosystems: effects of fire on soils and water. (2005).
45. Thomaz, E. Interaction between Ash and soil microaggregates reduces runoff and soil loss. *Sci. Total Environ.* **625**, 1257–1263 (2018).
46. Thomaz, E. Ash physical characteristics affects differently soil hydrology and erosion subprocesses. *Land. Degrad. Dev.* **29**, 690–700 (2018).
47. Schaap, M. G., Leij, F. J., Van Genuchten, M. T. & Brown, G. E. rosetta: a computer program for estimating soil hydraulic parameters with hierarchical Pedotransfer functions. *J. Hydrol. (Amst)*. **251**, 163–176 (2001).
48. R Core Team. R: A language and environment for statistical computing. R Foundation for Statistical Computing. Preprint at. (2021).
49. Wickham, H. et al. Welcome to the tidyverse. *J. Open. Source Softw.* **4**, 1686 (2019).
50. Wickman, H. *Ggplot2, Use R!* (Springer International Publishing, 2016). <https://doi.org/10.1007/978-3-319-24277-4>
51. Zambrano-Bigiarini, M. *Package 'HydroGOF'. Goodness-of-Fit Functions for Comparison of Simulated and Observed Hydrological Time Series (Version 0.6–0.1) [R Package Manual].* CRAN. (2024). <https://github.com/hzambran/hydroGOF>
52. Sonmez, S., Buyuktas, D., Okturen, F. & Citak, S. Assessment of different soil to water ratios (1:1, 1:2.5, 1:5) in soil salinity studies. *Geoderma* **144**, 361–369 (2008).
53. Weather Spark. Average Weather in La Ligua and Melipilla, Chile – Year Round. (2025). <https://weatherspark.com>

54. Schoeneberger, P., Wysocki, D. & Benham, E. *Field Book for Describing and Sampling Soils, Version 3.0.* (2021).
55. Duarte, T. F., Bonfim-Silva, E. M., da Silva, T. J. A., Koetz, M. & Lima, G. F. Physical-hydric properties of oxisol and Quartzipsamment associated with the application of wood Ash. *Revista Brasileira De Engenharia Agrícola E Ambiental.* **27**, 188–194 (2023).
56. Esmaelnejad, L., Shorafa, M., Gorji, M. & Hosseini, S. mossa. Impacts of Woody Biochar particle size on porosity and hydraulic conductivity of Biochar-Soil mixtures: an incubation study. *Commun. Soil. Sci. Plant. Anal.* **48**, 1710–1718 (2017).
57. Ibrahim, K. & Alghamdi, A. G. Available water capacity of sandy soils as affected by Biochar application: A meta-analysis. *Catena (Amst)* **214**, 106281 (2022).
58. Amewode, E. K. et al. Investigation of amended sandy soil's water retention characteristics. *Afr. J. Appl. Res.* **9**, 90–103 (2023).
59. Shaheen, S. M., Hooda, P. S. & Tsadilas, C. D. Opportunities and challenges in the use of coal fly ash for soil improvements - A review. *J. Environ. Manage.* **145**, 249–267 (2014). <https://doi.org/10.1016/j.jenvman.2014.07.005>
60. Zajac, G., Szyszlak-Barglowicz, J., Golębiowski, W. & Szczepanik, M. Chemical characteristics of biomass ashes. *Energies (Basel)* **11**, 2885,1–15 (2018).
61. Francos, M., Stefanuto, E. B., Úbeda, X. & Pereira, P. Long-term impact of prescribed fire on soil chemical properties in a wildland-urban interface. Northeastern Iberian Peninsula. *Sci. Total Environ.* **689**, 305–311 (2019).
62. Huang, J. & Hartemink, A. E. Soil and environmental issues in sandy soils. *Earth-Science Reviews.* **208**, (2020). <https://doi.org/10.1016/j.earscirev.2020.103295>
63. Souza-Alonso, P. et al. Post-fire ecological restoration in Latin American forest ecosystems: Insights and lessons from the last two decades. *For. Ecol. Manag.* **509**, (2022). <https://doi.org/10.1016/j.foreco.2022.120083>
64. González-Pelayo, O. et al. The effects of wildfire frequency on post-fire soil surface water dynamics. *Eur. J. Res.* **143**, 493–508 (2024).
65. Ministerio del Medio Ambiente. *Reglamento de Clasificación de Especies. Decreto Supremo N°64* (2024). <https://clasificacionespeci.es.mma.gob.cl/>, Chile.

Acknowledgements

E. Acuña thanks the support from the ANID Doctorado Nacional Scholarship N° 21200370, Government of Chile.

Author contributions

Edouard J. Acuña: Conceptualization, Data curation, Formal analysis, Investigation, Methodology, Visualization, Writing – original draft, Writing – review & editing. Carlos A. Bonilla: Conceptualization, Funding acquisition, Formal analysis, Investigation, Methodology, Project administration, Supervision, Visualization, Writing – review & editing.

Funding

This research was supported by funding from the National Agency for Research and Development, Chile, Grant ANID/FONDECYT/Regular 1191166.

Declarations

Competing interests

The authors declare no competing interests.

Experimental research with plants

This study complied with relevant institutional (Pontificia Universidad Católica de Chile) and national guidelines and legislation governing the use of plant material. *Q. saponaria* samples were collected from trees located within the San Joaquín Campus of the Pontificia Universidad Católica de Chile (Metropolitan Region), with institutional authorization. *Q. saponaria* is a native species and is not classified as protected or endangered under current Chilean environmental regulations⁶⁵ (Ministerio del Medio Ambiente, Gobierno de Chile). Therefore, no additional permits were required. A voucher specimen of *Q. saponaria* was deposited in the public Herbarium AGUCH (Herbario de la Facultad de Ciencias Agronómicas, Universidad de Chile), under accession number AGUCH-78820. Plant material of *E. globulus*, an exotic and widely cultivated species in Chile, was collected from trees growing along a public roadside (Route E-46, Zapallar, Valparaíso Region). In accordance with standard practice for non-native and widely cultivated plant species, voucher specimen deposition was not required for *E. globulus*. Both *E. globulus* and *Q. saponaria* specimens were identified based on their morphological characteristics by agricultural engineer Edouard J. Acuña.

Additional information

Correspondence and requests for materials should be addressed to C.A.B.

Reprints and permissions information is available at www.nature.com/reprints.

Publisher's note Springer Nature remains neutral with regard to jurisdictional claims in published maps and institutional affiliations.

Open Access This article is licensed under a Creative Commons Attribution-NonCommercial-NoDerivatives 4.0 International License, which permits any non-commercial use, sharing, distribution and reproduction in any medium or format, as long as you give appropriate credit to the original author(s) and the source, provide a link to the Creative Commons licence, and indicate if you modified the licensed material. You do not have permission under this licence to share adapted material derived from this article or parts of it. The images or other third party material in this article are included in the article's Creative Commons licence, unless indicated otherwise in a credit line to the material. If material is not included in the article's Creative Commons licence and your intended use is not permitted by statutory regulation or exceeds the permitted use, you will need to obtain permission directly from the copyright holder. To view a copy of this licence, visit <http://creativecommons.org/licenses/by-nc-nd/4.0/>.

© The Author(s) 2026